Geophysical Research Letters

RESEARCH LETTER
10.1029/2022GL100258

Key Points:

- Nitrate and nitric acid aerosol contribute significantly to the tropical upper troposphere and lower stratosphere (UTLS), Asian summer monsoon and polar regions
- The cold ambient conditions in the UTLS thermodynamically favor the condensation of nitric acid
- The simulated aerosol in the global UTLS is primarily composed of the secondarily formed nitrate, sulfate and organics

Supporting Information:

Supporting Information may be found in the online version of this article.

Correspondence to:

P. Yu,
pengfei.yu@colorado.edu

Citation:

Yu, P., Lian, S., Zhu, Y., Toon, O. B., Höpfner, M., & Borrmann, S. (2022). Abundant nitrate and nitric acid aerosol in the upper troposphere and lower stratosphere. *Geophysical Research Letters*, *49*, e2022GL100258. https://doi.org/10.1029/2022GL100258

Received 30 JUN 2022
Accepted 12 SEP 2022

Author Contributions:

Conceptualization: Pengfei Yu
Data curation: Michael Höpfner, Stephan Borrmann
Formal analysis: Pengfei Yu, Siying Lian, Owen B. Toon
Funding acquisition: Pengfei Yu
Investigation: Pengfei Yu, Yunqian Zhu, Owen B. Toon
Methodology: Pengfei Yu, Michael Höpfner, Stephan Borrmann
Project Administration: Pengfei Yu
Resources: Pengfei Yu
Supervision: Pengfei Yu
Validation: Pengfei Yu
Writing – original draft: Pengfei Yu
Writing – review & editing: Pengfei Yu, Siying Lian, Yunqian Zhu, Owen B. Toon, Michael Höpfner, Stephan Borrmann

Abundant Nitrate and Nitric Acid Aerosol in the Upper Troposphere and Lower Stratosphere

Pengfei Yu[1,2], Siying Lian[1,2], Yunqian Zhu[3,4], Owen B. Toon[3,5], Michael Höpfner[6], and Stephan Borrmann[7,8]

[1]Institute for Environmental and Climate Research, Jinan University, Guangzhou, China, [2]Guangdong–Hong Kong–Macau Joint Laboratory of Collaborative Innovation for Environmental Quality, Guangzhou, China, [3]Laboratory of Atmospheric and Space Sciences, University of Colorado, Boulder, Boulder, CO, USA, [4]National Center for Atmospheric Research, Boulder, CO, USA, [5]Department of Atmospheric and Oceanic Sciences, University of Colorado, Boulder, Boulder, CO, USA, [6]Institute of Meteorology and Climate Research, Karlsruhe Institute of Technology, Karlsruhe, Germany, [7]Johannes Gutenberg University, Mainz, Germany, [8]Max Planck Institute for Chemistry, Mainz, Germany

Abstract The tropospheric and stratospheric nitrate aerosol is simulated by a sectional aerosol model coupled to the Community Earth System Model. The simulated nitrate mass fractional contribution to aerosols is significantly higher in the upper troposphere and lower stratosphere (UTLS) than that at the surface. Both in situ measurements and simulations show that nitrate aerosol accounts for about 30%–40% of the aerosol mass at the tropopause of the Asian summer monsoon (ASM) region. Furthermore, simulated condensed nitric acid particles account for ∼20% of the annual mean aerosol mass at the tropical tropopause, and over 95% in the UTLS at the South Pole in June-July-August. Our study suggests that the extremely cold ambient conditions in the UTLS of the tropics, ASM and polar regions thermodynamically favor the condensation of ammonia and nitric acid. The widely distributed nitrate aerosol in the global UTLS may be overlooked by climate models.

Plain Language Summary The tropospheric and stratospheric nitrate aerosol is simulated by a sectional aerosol model coupled to the Community Earth System Model. Simulated nitrate aerosol mass concentrations are evaluated with observations at the surface and the upper troposphere and lower stratosphere (UTLS). At the global surface, simulated nitrate aerosols account for 6% of non-dust and non-sea salt aerosol mass. Significantly higher mass fractions of nitrate are simulated in the UTLS. Our study shows that nitrate accounts for about 30%–40% of the aerosol mass in the Asian tropopause aerosol layer. Furthermore, the model simulations suggested that condensed HNO_3 particles contribute to about 20% of the annual mean aerosol burden in the tropical tropopause layer and over 95% in the UTLS of the South Pole in June-July-August. We find that the cold conditions in the global UTLS thermodynamically favors the condensation of ammonia and nitric acid. The widely distributed nitrate aerosol in the global UTLS may be overlooked by climate models.

1. Introduction

Atmospheric nitrate particles are widely distributed in both the troposphere and the stratosphere. Under warm tropospheric conditions, pure nitric acid/water particles are difficult to form due to the high vapor pressure of HNO_3. Instead, ammonium nitrate (AN) aerosol (NH_4NO_3) can form with significantly lower vapor pressure. In the stratosphere, aerosol containing HNO_3 can form due to cold temperatures typically found during the polar night inside the polar vortex, where they are known as polar stratospheric clouds (PSCs). In PSC, the nitric acid can condense on the sulfate aerosol forming the supercooled ternary solution (STS) or remain in the solid-state as nitric acid trihydrate (NAT) particles. PSCs are critical for polar ozone depletion.

The temperature in the tropical tropopause layer (TTL) can be lower than 190 K. The cold ambient temperatures lower the vapor pressure and thermodynamically favor the condensation of the gaseous nitric acid onto the pre-existing aerosol (Hamill & Fiocco, 1988; Hervig & McHugh, 2002). The parameterization developed by Lin and Tabazadeh (2001) predicts that a significant portion of nitric acid in the upper troposphere and lower stratosphere (UTLS) can condense onto the particles irrespective of aerosol solution neutrality (i.e., ammonia-to-sulfate ratio). A narrow aerosol belt of NAT was revealed by in situ measurements in the TTL over Africa and South America (Jensen & Drdla, 2002; Popp et al., 2006; Voigt et al., 2007, 2008). The air in the TTL associated with cold temperatures is supersaturated with respect to NAT and the number concentration of NAT is less than $1.e^{-4}$ cm^{-3} with diameters between 1.7 and 6 μm (Popp et al., 2006; Voigt et al., 2008).

Höpfner et al. (2019) reported abundant nitrate in the UTLS of the Asian summer monsoon (ASM) region observed by airborne infrared remote limb-sounding, and satellite remote sounding using the Michelson Interferometer for Passive Atmospheric Sounding (MIPAS) satellite (Fischer et al., 2008). The infrared limb-sounding indicates that these nitrate particles are in the solid phase over the ASM region, which can potentially induce heterogeneous ice nucleation in the upper troposphere (Wagner et al., 2021). The in situ aerosol mass spectrometry measurements from the STRATOspheric and upper tropospheric processes for better CLIMate predictions (StratoClim) field campaign found that the mass concentration of nitrate is similar to organics in the UTLS of the ASM (Appel et al., 2022). The recent Cosmics Leaving OUtdoor Droplets experiment shows that under low temperatures (below 258 K), ammonia and nitric acid vapor can nucleate to form AN aerosols in the multi-acid solutions (HNO_3-H_2SO_4-NH_3) with a nucleation rate which is orders of magnitude higher than the pure HNO_3-NH_3 or H_2SO_4-NH_3 solutions (Wang et al., 2022).

The importance of nitrate aerosol in the global UTLS aerosol budget and their potential climate implications are still poorly understood. A computationally fast climate model capable of simulating the complex HNO_3-H_2SO_4-NH_3 system in both the warm (e.g., lower troposphere) and the cold (e.g., polar vortex, TTL, and ASM) environments is critically important to investigate the climate implications of the nitrate aerosol. In this study, we implement a whole atmosphere nitrate aerosol parameterization into the aerosol-climate model (CESM-CARMA) (Bardeen et al., 2008; Toon et al., 1988; Yu et al., 2015). Validations of the tropospheric nitrate aerosol model in warm environments are introduced in Text S1 and Figures S1–S4 of Supporting Information S1. Shown in Figures S5–S7 of Supporting Information S1, simulated nitrate accounts for ∼6% of the global annual mean non-sea salt and non-dust aerosol mass at the surface. In the study, we show that simulated nitrate mass fractional contribution aerosols are significantly higher in cold environments including the polar vortex (70–90°N/S), TTL (30°S–30°N) and ASM (20–40°N, 10–110°E) regions.

2. Methods

2.1. CESM/CARMA Climate Model

We use a sectional aerosol model, the Community Aerosol and Radiation Model for Atmospheres (CARMA) coupled with the Community Earth System Model (CESM-CARMA) (Bardeen et al., 2008; Toon et al., 1988; Yu et al., 2015, 2019), to study the spatial and temporal distributions of the nitrate aerosol in both troposphere and stratosphere. The model has 56 vertical layers from the surface up to 45 km with a vertical resolution of about 1 km in the UTLS. Simulations are run on a grid of 1.9° latitude × 2.5° longitude. The physical time step of CESM is 30 min. The model is nudged to the Goddard Earth Observing System version 5 analysis (GEOS-5). In the model runs, neither volcanic aerosol nor wildfire smoke aerosol are simulated. We run the model from 2017 to 2021 with an additional 2 years spin-up.

CARMA tracks two groups of aerosols: the first group is composed of pure sulfate with 20 discrete size bins ranging from 0.2 nm to 1.3 μm in radius; the other group is composed of internal mixtures of various aerosol components including mixed sulfate, organics, black carbon, dust, salt, ammonium, and nitrate. The mixed particles are divided into 20 discrete size bins ranging from 0.05 to 8.7 μm in radius (Yu et al., 2015). The secondary organics in both gas (SOG) and aerosol (SOA) phases are simulated based on the volatility-basis set parameterization developed by Pye et al. (2010). Five main species of SOG/SOA with the precursors of isoprene, monoterpene, xylene, benzene, and toluene are tracked in the model. Emission databases used for SO_2, VOCs, ammonia, primary organic aerosols and lightning NO are described by Emmons et al. (2010). The surface emission inventory of year 2015 is used in the study. The parameterizations of the sectional nitrate in the warm ($T > 235$K) and cold environments are described in Text S2 of Supporting Information S1.

2.2. Michelson Interferometer for Passive Atmospheric Sounding (MIPAS)

MIPAS measured atmospheric limb emission spectra in the thermal infrared region from 2002 until 2012 on board the polar orbiting satellite Envisat (Fischer et al., 2008). The infrared band of solid AN particles used for its detection and quantification of aerosol mass concentration is around 831 cm^{-1} (Höpfner et al., 2019; Wagner et al., 2021). Thus, because the measurements of MIPAS report solid AN aerosol, they can be treated as a lower limit of total aerosol nitrate. For the situation of the UTLS aerosol layer captured during StratoClim, though, AN retrieved from infrared limb-sounding matched the total nitrate observed by the airborne in-situ measurements (Höpfner et al., 2019).

2.3. Europe Research Council Instrument for the Chemical Composition of Aerosols (ERICA)

In July and August of 2017, an airborne European field campaign based in Kathmandu, Nepal (28°N, 84°E), named the stratospheric and upper tropospheric processes for better climate predictions (StratoClim), measured the atmospheric composition in the ASM region (Appel et al., 2022; Höpfner et al., 2019). The Geophysica high-altitude research aircraft carried a variety of instruments and reached up to 20 km during StratoClim. The in situ aerosol mass spectrometry using Europe Research Council Instrument for the Chemical Composition of Aerosols (ERICA) was implemented on the Geophysica (Hünig et al., 2022) during StratoClim. Aerosol compositions including nitrate, sulfate, organics and ammonium for particles with diameters between 0.11 and 3.5 μm were measured in real time by ERICA. Details of the instrument can be found in Hünig et al., 2022 and Appel et al. (2022).

3. Results

3.1. Nitrate in the Asian Summer Monsoon (ASM) Region

In the summer, a layer of aerosol in the ASM UTLS, named the Asian tropopause aerosol layer (ATAL) was observed by satellites (Vernier et al., 2015) and balloon-borne optical particle counters (Vernier et al., 2018; Yu et al., 2017). However, its chemical composition was not measured at the time the layer was described in these early studies. Previous global modeling studies suggest that sulfate, organics and nitrate are the most common aerosol species in the ATAL (Bossolasco et al., 2021; Fadnavis et al., 2017; Fairlie et al., 2020; Gu et al., 2016; Ma et al., 2019; Yu et al., 2015). Yu et al. (2015) predicted that secondary-formed organic aerosols account for about ∼70% of the ATAL mass budget, while sulfate accounts for ∼30%. Consistently, an enhancement of organic aerosol was observed in the ASM UTLS in July and August of 2017 during the StratoClim field campaign as shown in Figure 1a (Appel et al., 2022). In addition to organics and sulfate, abundant nitrate aerosol was previously predicted by climate models (Fairlie et al., 2020; Gu et al., 2016; Ma et al., 2019). Recently nitrate aerosol was observed in the ATAL and accounted for about one third of the ATAL mass during the StratoClim. Shown in Figure 1b, similar aerosol compositions in the ATAL region are simulated by the CESM-CARMA model described here. Both measured and modeled sulfate mass concentration are in units of micrograms per unit cubic meters in the standard air. The mass concentration of sulfate in standard air increased with altitude from the troposphere to the stratosphere and accounted about 15%–30% of total aerosol mass in ATAL. Sulfate concentration increases with altitudes from UT to the stratosphere due to the stratospheric sulfur source originating from carbonyl sulfide. Different from sulfate, both organics and nitrate aerosol peaked near the tropopause, suggesting the in-situ formation in the UTLS region. The occurrence of widespread and intense new particle formation events in the UTLS of ASM has been observed from in-situ measurements by Weigel et al. (2021) even inside anvil outflow clouds. Both simulations with the model described here and observations suggest that nitrate contributes about 30%–40% of the aerosol mass in ATAL (Figure 1b). Similar nitrate concentrations (∼0.5–0.6 μg m^{-3} in the standard air near the tropopause) are also simulated by Fairlie et al. (2020), Gu et al. (2016), and Ma et al. (2019).

In general, simulated total aerosol mass abundance in the ATAL region is about 30% smaller than observations as shown in Figures 1a and 1b. Simulations in Figure 1b underestimate the nitrate aerosol concentrations from 10 to 14 km compared with observations, which may indicate that the model underestimates the convective transport and surface emissions of ammonia, which might stabilize the nitrate. Simulated nitrate aerosols in ATAL are mostly composed of condensed HNO_3 particles, which can form near the cold tropopause and evaporate at warmer altitudes. Note that the measured variability of aerosol concentration in ASM on the flight-to-flight basis during the StratoClim field campaign is large because the dynamics of the anticyclone is highly variable (Appel et al., 2022). For example, the 25th and 75th percentiles of the nitrate concentration measured during the entire StratoClim field campaign are about 0.5–1.5 μg m^{-3} in the standard air for ATAL region and about 0.006–0.27 μg m^{-3} in the standard air between 10 and 14 km (Appel et al., 2022).

Consistent with the in-situ aerosol mass spectrometry measurements by ERICA in 2017 (Appel et al., 2022), Höpfner et al. (2019) reported a climatological nitrate aerosol peak in the ATAL from years 2002 to 2011 based on MIPAS satellite observations. The nitrate observed by MIPAS was in the form of solid AN particles. Shown in Figure 1c, both the AN particles in MIPAS satellite data (Höpfner et al., 2019) and the condensed HNO_3 particles simulated by CESM-CARMA peak near August with the monthly mean temperature close to 200K. The cold ambient environment thermodynamically favored the condensation of nitrate aerosol in this altitude region

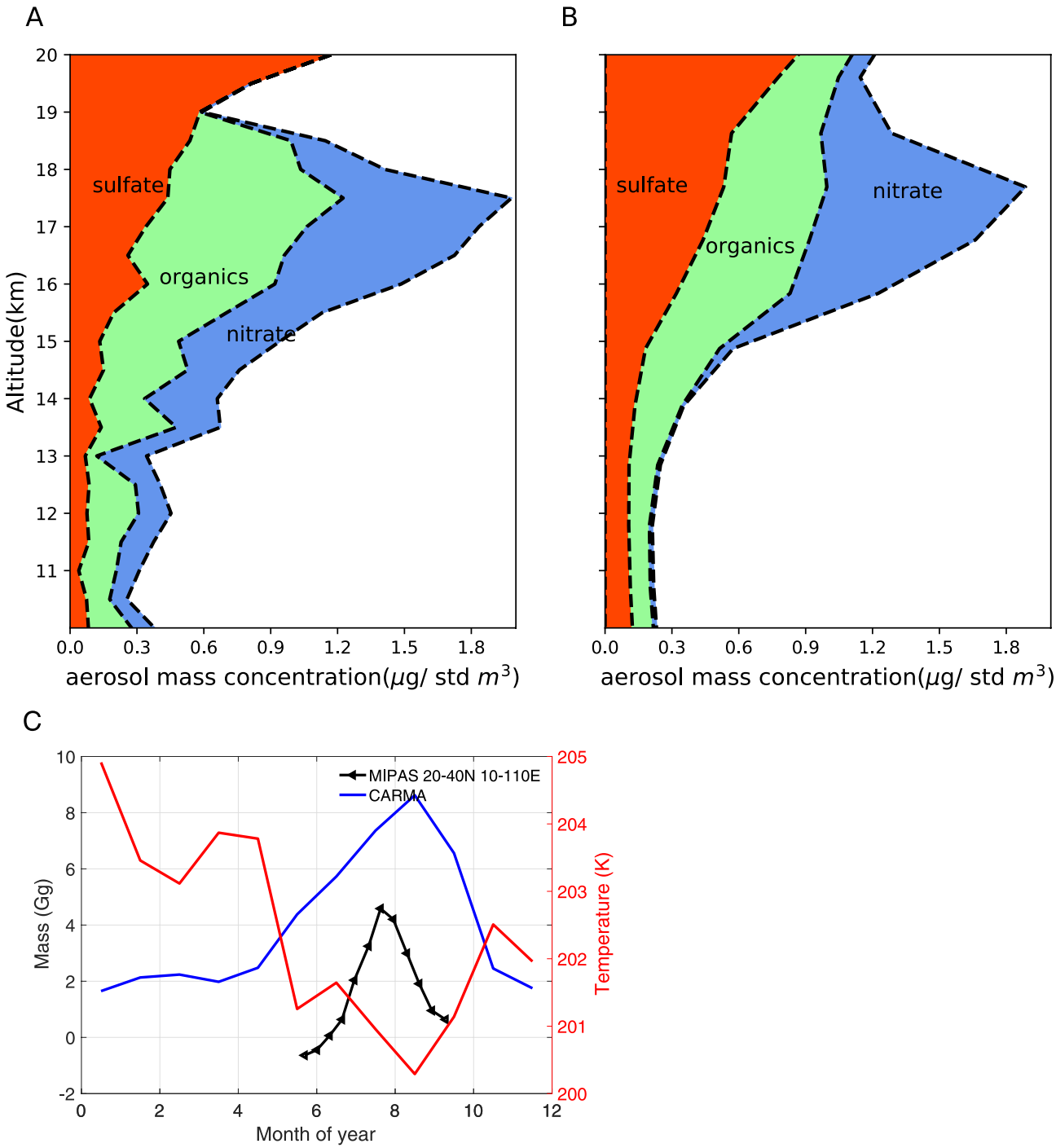

Figure 1. (a) Vertical distribution of the aerosol compositions measured by the Europe Research Council Instrument for the Chemical Composition of Aerosols (ERICA) instrument during the StratoClim field campaign in August of 2017 (Appel et al., 2022; Höpfner et al., 2019). Nitrate, organics and sulfate are denoted by the color-coded stacked regions. Observations are averages of all eight flights in StratoClim field campaign; (b) same as A but for the simulated aerosol composition by Community Earth System Model-CARMA in August of 2017; (c) Simulated monthly mean total nitrate and nitric acid aerosol mass in the upper troposphere and lower stratosphere of Asian monsoon region (20–40°N, 10–110°E, 13–17 km) is shown in the blue line; observations of nitrate in the form of solid ammonium nitrate by the Michelson Interferometer for Passive Atmospheric Sounding (MIPAS) satellite is shown in black line with triangles (Höpfner et al., 2019); simulated temperature vertical distribution is shown by the red line (right axis). Aerosol mass concentrations are in unit of microgram per unit cubic meters in the standard air (std) for all panels.

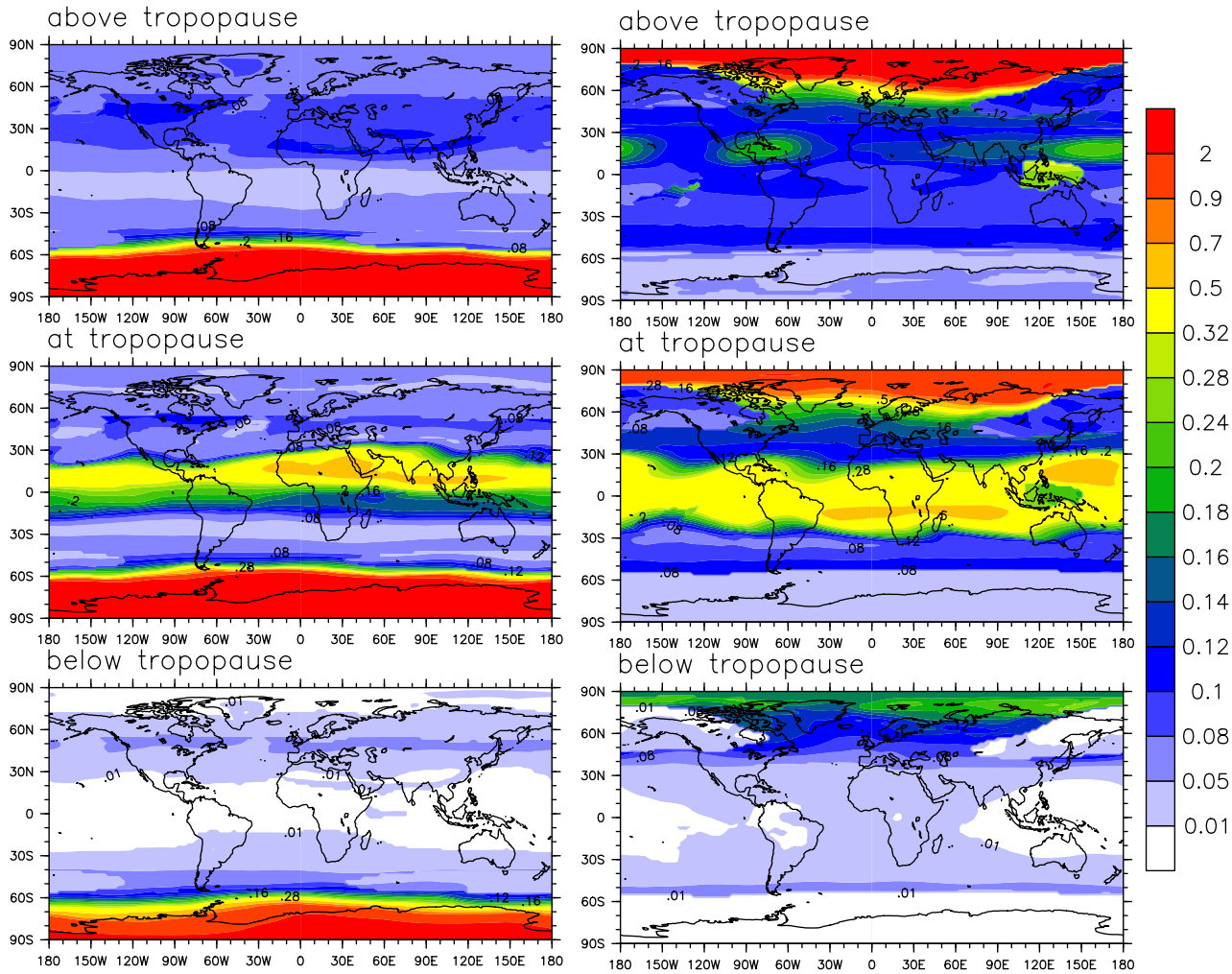

Figure 2. (left) Simulated mass concentration (unit: μg m^{-3} in the standard air) of nitrate 2 km above the tropopause (first row), at tropopause (second row) and 2 km below the tropopause (third row) in June-July-Aug averaged from year 2019–2021; (right) same as left but for December-January-February averaged from year 2019–2021.

because the vapor pressure of nitric acid decreases with temperature exponentially (Lin & Tabazadeh, 2001). In addition, a higher amount of ammonia is transported to the upper troposphere in June-July-August (JJA) than in other months (Höpfner et al., 2016, 2019) tied with the high surface emissions (Warner et al., 2017) and the high convective activity in the ASM region. The lofted ammonia remains in the condensed phase in the extremely cold environment and stabilizes the nitrate aerosol in the condensed phase.

The simulated nitrate aerosols in the ASM region are condensed HNO_3 particles that reside mostly south of 30°N (Figure 2). MIPAS satellite data shows the solid AN particles peak around 20–30°N and remain elevated at 40°N (Höpfner et al., 2019). The model probably fails to simulate the observed AN aerosol due to underestimation of ammonia emissions in the Asian monsoon region especially in Eastern and Central China. MIPAS detected no solid-state AN in the ATAL region from October to the next June (Höpfner et al., 2019). However, modeled nitrate aerosol in the chemical forms of HNO_3 and NH_4NO_3 persists throughout the year with the lowest mass still greater than 1 Gg in the ASM UTLS. Note, the phases (solid or liquid) of the particles are not explicitly calculated in the current model.

3.2. Nitric Acid Aerosol in the Tropical Tropopause Layer (TTL) and the Polar Vortex

The cold ambient environment in the global UTLS as well as ammonia transported via deep convection that lowers the vapor pressure of nitric acid both enhance the formation of nitrate in the condensed phase (Lin &

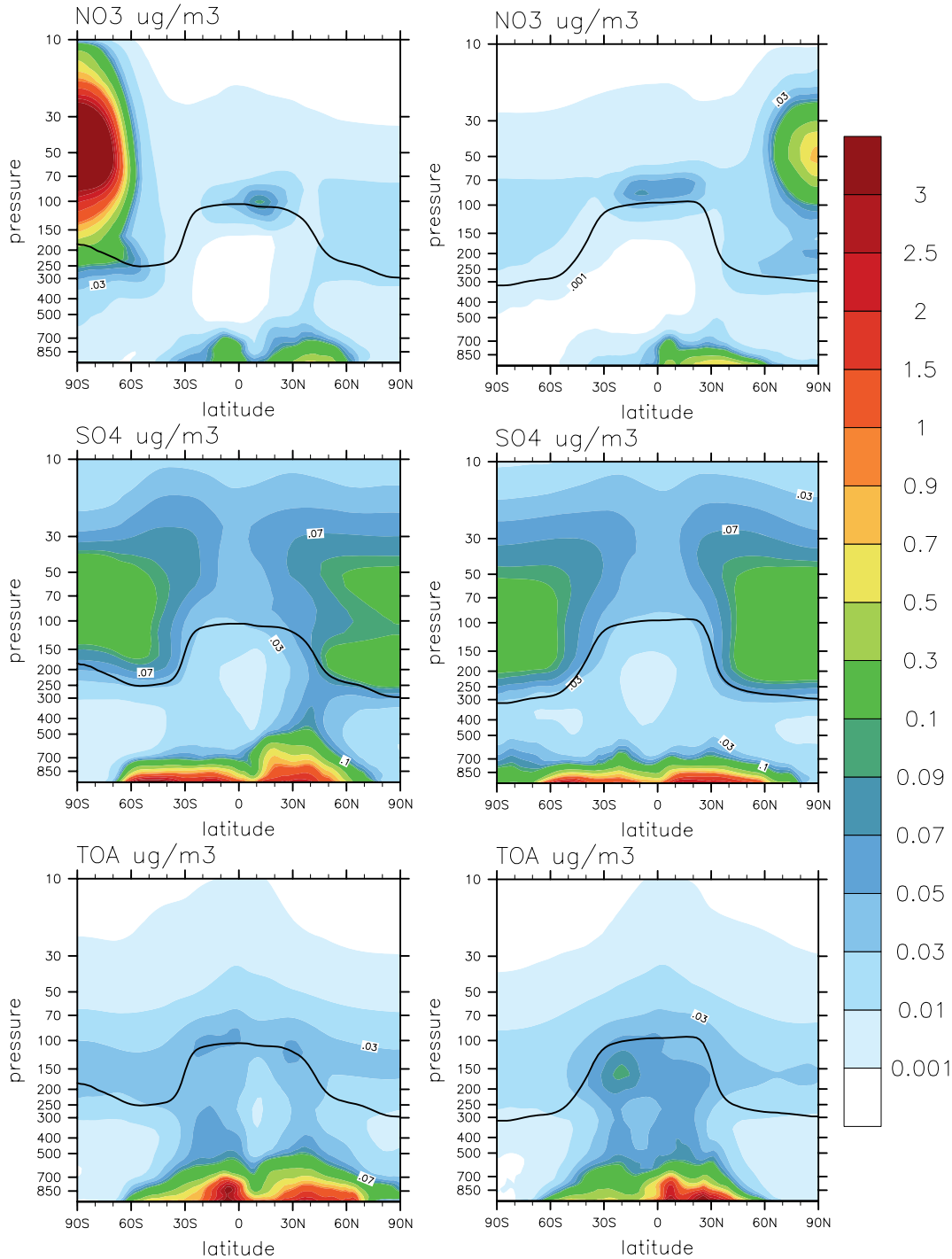

Figure 3. (left) Simulated zonal averaged aerosol (nitrate, sulfate and organics) mass concentrations in June-July-August (JJA) averaged from year 2019–2021. The black solid line on each panel denotes the simulated tropopause height averaged in JJA of 2019–2021; (right) same as (left) but for December-January-February.

Tabazadeh, 2001). In Figures 2 and 3, simulated nitrate is distributed in a thin layer about 2 and 3 km deep near the tropical tropopause where the temperature is coldest. This simulated shallow nitrate aerosol layer is mostly composed of condensed HNO_3 particles in cold temperatures. In situ measurements (Jensen & Drdla, 2002; Popp et al., 2006; Voigt et al., 2007, 2008) show that the HNO_3 particles in the TTL are of low number density ($<10^{-4}$ cm^{-3}) and large in size (1.7–6 μm in diameter). This implies a nitrate concentration of

about 0.004–0.17 μg m^{-3} in standard air. Inconsistently, satellites data imply concentrations of about from 12 to 40 μg m^{-3} in standard air (Hervig & McHugh, 2002). Simulated concentrations of the condensed HNO_3 particles are about 0.3 μg m^{-3} at the TTL, which is close to the upper bound of airborne measurements, and about a factor of 40–130 smaller than satellite data (Hervig & McHugh, 2002). Shown in Figure 2, modeled nitrate aerosol is depleted 2 km above or below the tropical tropopause. However, the simulated organics remain elevated 2 km above or below the tropical tropopause (Figure 3).

In JJA, the simulated nitrate is abundant in the TTL and in the ASM region. Consistent with the observed aerosol composition near Nepal (Figure 1), organics and nitrate in the ATAL have similar abundances. The simulated longitudinal gradient of nitrate from the central ASM region to the oceanic basins in the NH mid-latitude UTLS is about a factor of 5, as shown in Figure 2. Since organics are not sensitive to temperature, their concentrations are more uniform with longitude than the concentrations of nitrates, as shown in Figure S8 of Supporting Information S1. As shown in Figure S8 of Supporting Information S1, the modeled ammonium at the NH tropopause is about a factor of 2 higher than in the Southern Hemisphere due to higher anthropogenic precursors emissions (e.g., ammonia) in NH. Simulated ammonium aerosol is elevated in the ASM region in JJA due to high convective activity. Ammonium stabilizes the nitrate so that it is less dependent on low temperatures than HNO_3.

As the temperature decreases in polar regions, nitric acid condenses on sulfate aerosol and forms the STS (Type Ib PSCs). Both sulfate aerosol, especially when it is elevated by volcanic eruptions, and STS provide large surface area for the heterogeneous reactions that convert inactive chlorine and bromine ($ClONO_2$ and HCl; $BrONO_2$, and HBr) into photochemically active chlorine and bromine (Solomon et al., 1986). Nitric acid trihydrate (NAT, Type Ia PSCs) composes solid phase PSCs. Large NAT particles dominate denitrification, reducing NO_y and thereby slowing the reformation of chlorine and bromine reservoirs (Fahey et al., 2001; Lambert et al., 2012; Toon et al., 1986, 1990; Waibel et al., 1999). Shown in Figure 3, the condensed phase nitrate in the South Polar Vortex (SPV) and North Polar Vortex (NPV) during their wintertime form PSCs with peaks located around 50 mb. PSCs in the SPV are more homogeneous and more abundant than in the NPV because the SPV is colder and more stable in Antarctic winter. PSCs are most abundant in the NPV over Scandinavia where mountain waves cause frequent adiabatic cooling.

3.3. Nitrate (Ion and Nitric Acid), Sulfate and Organics' Budget in Global UTLS

Figures 4a and 4b illustrate the simulated latitudinal distribution of the relative mass fractions of nitrate, sulfate and organics in the UTLS in JJA and December-January-February (DJF) seasons. The simulated column density of sulfate is higher in the mid-high latitudes than in the tropics. On the contrary, the simulated organics column density peaks in the tropics as a result of the larger amount of biogenic emissions and faster gas-particle partitioning from organic vapor to the secondary organic aerosol solution in the TTL (Tilmes et al., 2019; Yu et al., 2015). Simulated nitrate is more abundant in cold ambient conditions including the TTL and the winter poles. The simulated nitrate aerosol (in the form of nitrate ion or nitric acid) contributes ∼20% of the annual mean aerosol mass budget in the TTL (Figure 4b). In the winter poles, nitrate's mass contribution increases as nitric acid gas condenses in the cold environments. In JJA over Antarctica, simulated condensed HNO_3 particles associated with PSCs dominates with a mass contribution greater than 95% (Figure 4e); while in DJF of North Pole, the condensed HNO_3 particle accounts for 60% of aerosol mass budget (Figure 4f). Organic aerosol contributes ∼40% of the annual mean aerosol mass in the tropics (Figure 4c) and sulfate contributes ∼70% in the mid-latitudes (Figure 4d). In the mid-stratosphere, a layer of aerosol (Junge & Manson, 1961) is also simulated (not shown), which is primarily OCS derived sulfate aerosols.

4. Summary

Our manuscript presents a global modeling study of the atmospheric HNO_3-H_2SO_4-NH_3 system in both the troposphere (warm environment) and the stratosphere (cold environment). Previously it was thought that the UTLS aerosol was mainly composed of secondary sulfate and organics (Froyd et al., 2009; Murphy et al., 2014; Yu et al., 2015, 2016). Our model suggests that nitrate aerosol contributes about 30%–40% of total aerosol mass in ATAL. Moreover, we find that condensed HNO_3 particles contribute ∼20% to the annual mean total aerosol mass in the TTL. The nitric acid particles dominate the mass in the PSCs in the South Pole. The extremely cold ambient conditions in the UTLS of the tropics, Asian summer monsoon and polar regions thermodynamically

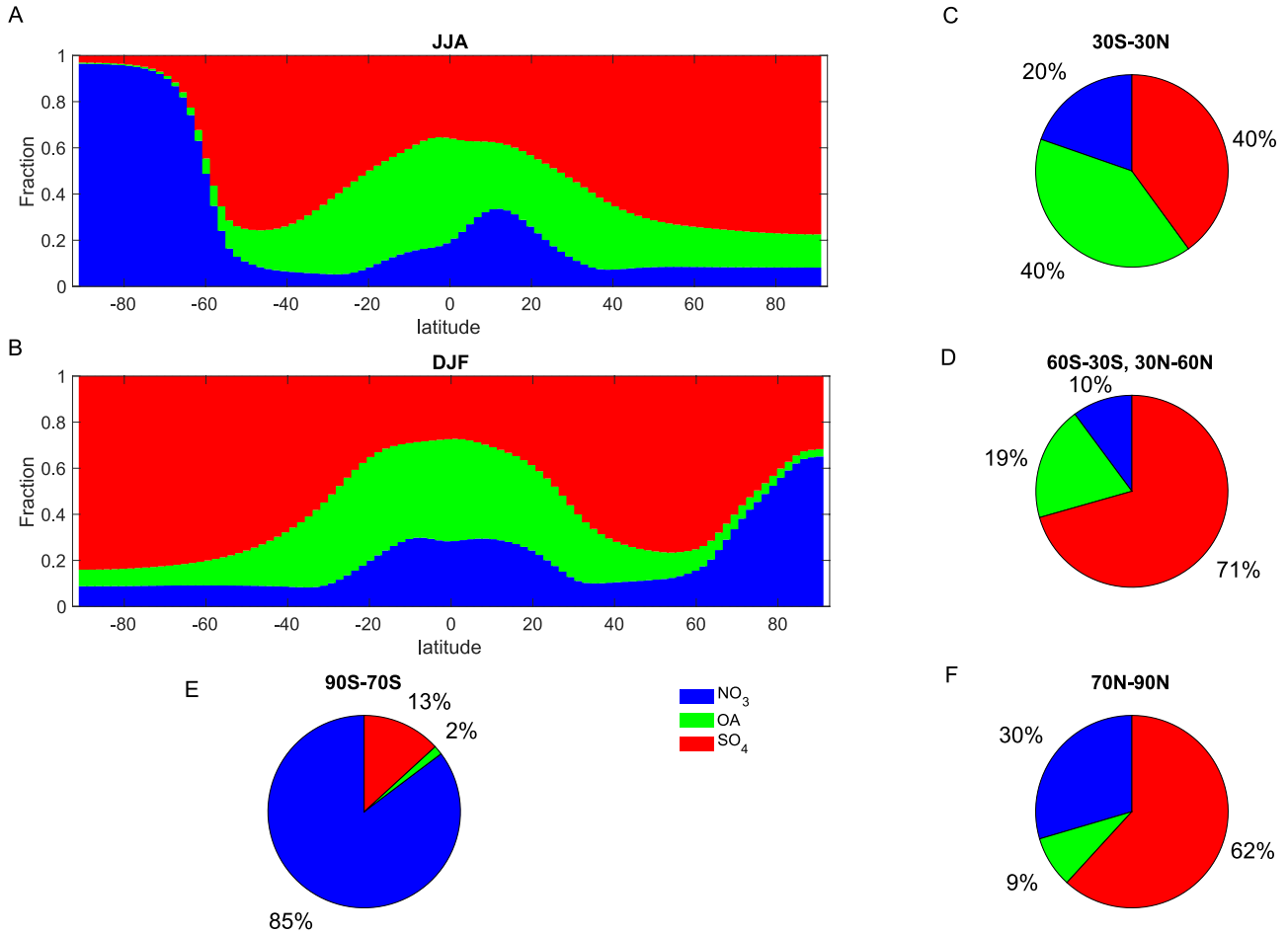

Figure 4. (a) Simulated latitudinal distribution of the mass fraction of three secondary aerosols (nitrate, organics and sulfate) in the upper troposphere and lower stratosphere (UTLS) (50–140 mb) averaged in June-July-August (JJA) of year 2021; (b) same as A but averaged in December-January-February of year 2021; (c) simulated annual mean mass fraction of three secondary aerosols in tropical UTLS between 50 and 140 mb; (d) same as (c) but for mid-latitudes in both hemispheres; (e) same (c) but for South Pole; (f) same as (c) but for North Pole.

favor the condensation of ammonia and nitric acid. Our study highlights the important but potentially overlooked role of nitrate aerosol in the three extreme cold environments in the UTLS. Our study calls for evaluations of the change of UTLS nitrate and nitric acid aerosols under anthropogenic influences and their implications for radiative forcing and stratospheric ozone.

Conflict of Interest

The authors declare no conflicts of interest relevant to this study.

Data Availability Statement

MIPAS data is available at from the KITopen archive at https://doi.org/10.5445/IR/1000095498; IMPROVE data is available from https://vista.cira.colostate.edu/Improve/improve-data/; EMEP data is available at https://ebas-data.nilu.no/; EANET data is available from https://monitoring.eanet.asia/document/public/index; model simulations are available at https://doi.org/10.17605/OSF.IO/YMG6R.

Acknowledgments
The CESM project is supported by the National Science Foundation and the Office of Science (BER) of the U.S. Department of Energy. The authors acknowledge high-performance computing support from Cheyenne (doi.org/10.5065/D6RX99HX) provided by NCAR's Computational and Information Systems Laboratory, sponsored by the National Science Foundation. This work is supported by the National Natural Science Foundation of China (42175089) and the second Tibetan Plateau Scientific Expedition and Research Program (STEP, 2019QZKK0604). S.L. is supported by the National Natural Science Foundation of China (42121004). OBT and YZ were supported by NSF Award 1853932. SB acknowledges financial support from the German Research Foundation (DFG), SFB/TR-301 (TPChange, Project-ID 428312742, Project A4) and the DFG funded Joint Sino-German Research Project BO 1829/12-1.

References

Appel, O., Appel, O., Köllner, F., Dragoneas, A., Hünig, A., Molleker, S., et al. (2022). Chemical analysis of the Asian Tropopause Aerosol Layer (ATAL) with emphasis on secondary aerosol particles using aircraft based in-situ aerosol mass spectrometry. *Atmospheric Chemistry and Physics*, *2022*, 1–37. https://doi.org/10.5194/acp-2022-92

Bardeen, C. G., Toon, O. B., Jensen, E. J., Marsh, D. R., & Harvey, V. L. (2008). Numerical simulations of the three-dimensional distribution of meteoric dust in the mesosphere and upper stratosphere. *Journal of Geophysical Research*, *113*, D17202. https://doi.org/10.1029/2007jd009515

Bossolasco, A., Jegou, F., Sellitto, P., Berthet, G., Kloss, C., & Legras, B. (2021). Global modeling studies of composition and decadal trends of the Asian Tropopause Aerosol Layer. *Atmospheric Chemistry and Physics*, *21*(4), 2745–2764. https://doi.org/10.5194/acp-21-2745-2021

Emmons, L. K., Walters, S., Hess, P. G., Lamarque, J.-F., Pfister, G. G., Fillmore, D., et al. (2010). Description and evaluation of the model for ozone and related chemical tracers, version 4 (MOZART-4). *Geoscientific Model Development*, *3*(1), 43–67. https://doi.org/10.5194/gmd-3-43-2010

Fadnavis, S., Kalita, G., Kumar, K. R., Gasparini, B., & Li, J.-L. F. (2017). Potential impact of carbonaceous aerosol on the upper troposphere and lower stratosphere (UTLS) and precipitation during Asian summer monsoon in a global model simulation. *Atmospheric Chemistry and Physics*, *17*(18), 11637–11654. https://doi.org/10.5194/acp-17-11637-2017

Fahey, D. W., Gao, R. S., Carslaw, K. S., Kettleborough, J., Popp, P. J., Northway, M. J., et al. (2001). The detection of large HNO3-containing particles in the winter Arctic stratosphere. *Science*, *291*(5506), 1026–1031. https://doi.org/10.1126/science.1057265

Fairlie, T. D., Liu, H., Vernier, J.-P., Campuzano-Jost, P., Jimenez, J. L., Jo, D. S., et al. (2020). Estimates of regional source contributions to the Asian tropopause aerosol layer using a chemical transport model. *Journal of Geophysical Research: Atmospheres*, *125*, e2019JD031506. https://doi.org/10.1029/2019JD031506

Fischer, H., Birk, M., Blom, C., Carli, B., Carlotti, M., von Clarmann, T., et al. (2008). MIPAS: An instrument for atmospheric and climate research. *Atmospheric Chemistry and Physics*, *8*(8), 2151–2188. https://doi.org/10.5194/acp-8-2151-2008

Froyd, K. D., Murphy, D. M., Sanford, T. J., Thomson, D. S., Wilson, J. C., Pfister, L., & Lait, L. (2009). Aerosol composition of the tropical upper troposphere. *Atmospheric Chemistry and Physics*, *9*(13), 4363–4385. https://doi.org/10.5194/acp-9-4363-2009

Gu, Y., Liao, H., & Bian, J. (2016). Summertime nitrate aerosol in the upper troposphere and lower stratosphere over the Tibetan Plateau and the South Asian summer monsoon region. *Atmospheric Chemistry and Physics*, *16*(11), 6641–6663. https://doi.org/10.5194/acp-16-6641-2016

Hamill, P., & Fiocco, G. (1988). Nitric acid aerosols at the tropical tropopause. *Geophysical Research Letters*, *15*(11), 1189–1192. https://doi.org/10.1029/GL015i011p01189

Hervig, M., & McHugh, M. (2002). Tropical nitric acid clouds. *Geophysical Research Letters*, *29*(7), 1125. https://doi.org/10.1029/2001GL014271

Höpfner, M., Ungermann, J., Borrmann, S., Wagner, R., Spang, R., Riese, M., et al. (2019). Ammonium nitrate particles formed in upper troposphere from ground ammonia sources during Asian monsoons. *Nature Geoscience*, *12*(8), 608–612. https://doi.org/10.1038/s41561-019-0385-8

Höpfner, M., Volkamer, R., Grabowski, U., Grutter, M., Orphal, J., Stiller, G., et al. (2016). First detection of ammonia (NH3) in the Asian summer monsoon upper troposphere. *Atmospheric Chemistry and Physics*, *16*(22), 14357–14369. https://doi.org/10.5194/acp-16-14357-2016

Hünig, A., Appel, O., Dragoneas, A., Molleker, S., Clemen, H.-C., Helleis, F., et al. (2022). Design, characterization, and first field deployment of a novel aircraft-based aerosol mass spectrometer combining the laser ablation and flash vaporization techniques. *Atmospheric Measurement Techniques*, *15*(9), 2889–2921. https://doi.org/10.5194/amt-15-2889-2022

Jensen, E., & Drdla, K. (2002). Nitric acid concentrations near the tropical tropopause: Implications for the properties of tropical nitric acid trihydrate clouds. *Geophysical Research Letters*, *29*(20), 62-1–62-4. https://doi.org/10.1029/2002GL015190

Junge, C. E., & Manson, J. E. (1961). Stratospheric aerosol studies. *Journal of Geophysical Research*, *66*(7), 2163–2182. https://doi.org/10.1029/JZ066i007p02163

Lambert, A., Santee, M. L., Wu, D. L., & Chae, J. H. (2012). A-train CALIOP and MLS observations of early winter Antarctic polar stratospheric clouds and nitric acid in 2008. *Atmospheric Chemistry and Physics*, *12*(6), 2899–2931. https://doi.org/10.5194/acp-12-2899-2012

Lin, J. S., & Tabazadeh, A. (2001). A parameterization of an aerosol physical chemistry model for the NH3/H2SO4/HNO3/H2O system at cold temperatures. *Journal of Geophysical Research*, *106*(D5), 4815–4829. https://doi.org/10.1029/2000JD900598

Ma, J., Brhl, C., He, Q., Steil, B., Karydis, V. A., Klingmller, K., et al. (2019). Modeling the aerosol chemical composition of the tropopause over the Tibetan Plateau during the Asian summer monsoon. *Atmospheric Chemistry and Physics*, *19*(17), 11587–11612. https://doi.org/10.5194/acp-19-11587-2019

Murphy, D. M., Froyd, K. D., Schwarz, J. P., & Wilson, J. C. (2014). Observations of the chemical composition of stratospheric aerosol particles. *Quarterly Journal of the Royal Meteorological Society*, *140*(681), 1269–1278. https://doi.org/10.1002/qj.2213

Popp, P. J., Marcy, T. P., Jensen, E. J., Karcher, B., Fahey, D. W., Gao, R. S., et al. (2006). The observation of nitric acid-containing particles in the tropical lower stratosphere. *Atmospheric Chemistry and Physics*, *6*(3), 601–611. https://doi.org/10.5194/acp-6-601-2006

Pye, H. O. T., Chan, A. W. H., Barkley, M. P., & Seinfeld, J. H. (2010). Global modeling of organic aerosol: The importance of reactive nitrogen (NO_x and NO_3). *Atmospheric Chemistry and Physics*, *10*(22), 11261–11276. https://doi.org/10.5194/acp-10-11261-2010

Solomon, S., Garcia, R. R., Rowland, F. S., & Wuebbles, D. J. (1986). On the depletion of Antarctic ozone. *Nature*, *321*(6072), 755–758. https://doi.org/10.1038/321755a0

Tilmes, S., Hodzic, A., Emmons, L. K., Mills, M. J., Gettelman, A., Kinnison, D. E., et al. (2019). Climate forcing and trends of organic aerosols in the community Earth system model (CESM2). *Journal of Advances in Modeling Earth Systems*, *11*(12), 4323–4351. https://doi.org/10.1029/2019MS001827

Toon, O. B., Hamill, P., Turco, R. P., & Pinto, J. (1986). Condensation of HNO_3 and HCl in the winter polar stratospheres. *Geophysical Research Letters*, *13*(12), 1284–1287. https://doi.org/10.1029/GL013i012p01284

Toon, O. B., Turco, R. P., & Hamill, P. (1990). Denitrification mechanisms in the polar stratospheres. *Geophysical Research Letters*, *17*(4), 445–448. https://doi.org/10.1029/GL017i004p00445

Toon, O. B., Turco, R. P., Westphal, D., Malone, R., & Liu, M. (1988). A multidimensional model for aerosols—Description of computational analogs. *Journal of the Atmospheric Sciences*, *45*(15), 2123–2144. https://doi.org/10.1175/1520-0469(1988)045<2123:AMMFAD>2.0.CO;2

Vernier, J. P., Fairlie, T. D., Deshler, T., Venkat Ratnam, M., Gadhavi, H., Kumar, B. S., et al. (2018). BATAL: The balloon measurement campaigns of the Asian tropopause aerosol layer. *Bulletin of the American Meteorological Society*, *99*(5), 955–973. https://doi.org/10.1175/BAMS-D-17-0014.1

Vernier, J. P., Fairlie, T. D., Natarajan, M., Wienhold, F. G., Bian, J., Martinsson, B. G., et al. (2015). Increase in upper tropospheric and lower stratospheric aerosol levels and its potential connection with Asian pollution. *Journal of Geophysical Research: Atmospheres*, *120*, 1608–1619. https://doi.org/10.1002/2014JD022372

Voigt, C., Kaercher, B., Schlager, H., Schiller, C., Kraemer, M., de Reus, M., et al. (2007). In situ observations and modeling of small nitric acid-containing ice crystals. *Atmospheric Chemistry and Physics*, *7*(12), 3373–3383. https://doi.org/10.5194/acp-7-3373-2007

Voigt, C., Schlager, H., Roiger, A., Stenke, A., de Reus, M., Borrmann, S., et al. (2008). Detection of reactive nitrogen containing particles in the tropopause region—Evidence for a tropical nitric acid trihydrate (NAT) belt. *Atmospheric Chemistry and Physics*, *8*(24), 7421–7430. https://doi.org/10.5194/acp-8-7421-2008

Wagner, R., Testa, B., Höpfner, M., Kiselev, A., Mohler, O., Saathoff, H., et al. (2021). High-resolution optical constants of crystalline ammonium nitrate for infrared remote sensing of the Asian tropopause aerosol layer. *Atmospheric Measurement Techniques*, *14*(3), 1977–1991. https://doi.org/10.5194/amt-14-1977-2021

Waibel, A. E., Peter, T., Carslaw, K. S., Oelhaf, H., Wetze, G., Crutzen, P. J., et al. (1999). Arctic ozone loss due to denitrification. *Science (New York, N.Y.)*, *283*(5410), 2064–2069. https://doi.org/10.1126/science.283.5410.2064

Wang, M., Xiao, M., Bertozzi, B., Marie, G., Rorup, B., Schulze, B., et al. (2022). Synergistic HNO_3-H_2SO_4-NH_3 upper tropospheric particle formation. *Nature*, *605*(7910), 483–489. https://doi.org/10.1038/s41586-022-04605-4

Warner, J. X., Dickerson, R. R., Wei, Z., Strow, L. L., Wang, Y., & Liang, Q. (2017). Increased atmospheric ammonia over the world's major agricultural areas detected from space. *Geophysical Research Letters*, *44*(6), 2875–2884. https://doi.org/10.1002/2016GL072305

Weigel, R., Mahnke, C., Baumgartner, M., Kramer, M., Spichtinger, P., Spelten, N., et al. (2021). In situ observation of new particle formation (NPF) in the tropical tropopause layer of the 2017 Asian monsoon anticyclone—Part 2: NPF inside ice clouds. *Atmospheric Chemistry and Physics*, *21*(17), 13455–13481. https://doi.org/10.5194/acp-21-13455-2021

Yu, P., Murphy, D. M., Portmann, R. W., Toon, O. B., Froyd, K. D., Rollins, A. W., et al. (2016). Radiative forcing from anthropogenic sulfur and organic emissions reaching the stratosphere. *Geophysical Research Letters*, *43*(17), 9361–9367. https://doi.org/10.1002/2016GL070153

Yu, P., Toon, O. B., Bardeen, C. G., Mills, M. J., Fan, T., English, J. M., & Neely, R. R. (2015). Evaluations of tropospheric aerosol properties simulated by the community Earth system model with a sectional aerosol microphysics scheme. *Journal of Advances in Modeling Earth Systems*, *7*(2), 865–914. https://doi.org/10.1002/2014MS000421

Yu, P. F., Froyd, K. D., Portmann, R. W., Toon, O. B., Freitas, S. R., Bardeen, C. G., et al. (2019). Efficient in-cloud removal of aerosols by deep convection. *Geophysical Research Letters*, *46*(2), 1061–1069. https://doi.org/10.1029/2018GL080544

Yu, P. F., Rosenlof, K. H., Liu, S., Telg, H., Thornberry, T. D., Rollins, A. W., et al. (2017). Efficient transport of tropospheric aerosol into the stratosphere via the Asian summer monsoon anticyclone. *Proceedings of the National Academy of Sciences*, *114*(27), 6972–6977. https://doi.org/10.1073/pnas.1701170114

References From the Supporting Information

Bian, H., Chin, M., Hauglustaine, D. A., Schulz, M., Myhre, G., Bauer, S. E., et al. (2017). Investigation of global particulate nitrate from the AeroCom phase III experiment. *Atmospheric Chemistry and Physics*, *17*(21), 12911–12940. https://doi.org/10.5194/acp-17-12911-2017

Bian, H. S., & Zender, C. S. (2003). Mineral dust and global tropospheric chemistry: Relative roles of photolysis and heterogeneous uptake. *Journal of Geophysical Research*, *108*(D21), 4672. https://doi.org/10.1029/2002JD003143

Feng, Y., & Penner, J. E. (2007). Global modeling of nitrate and ammonium: Interaction of aerosols and tropospheric chemistry. *Journal of Geophysical Research*, *112*, D01304. https://doi.org/10.1029/2005JD006404

Luo, B., Carslaw, K. S., Peter, T., & Clegg, S. L. (1995). Vapour pressures of H_2SO_4/HNO_3/HCl/HBr/H_2O solutions to low stratospheric temperatures. *Geophysical Research Letters*, *22*(3), 247–250. https://doi.org/10.1029/94GL02988

Malm, W. C., Schichtel, B. A., Pitchford, M. L., Ashbaugh, L. L., & Eldred, R. A. (2004). Spatial and monthly trends in speciated fine particle concentration in the United States. *Journal of Geophysical Research*, *109*, D03306. https://doi.org/10.1029/2003JD003739

Zaveri, R. A., Easter, R. C., Fast, J. D., & Peters, L. K. (2008). Model for simulating aerosol interactions and chemistry (MOSAIC). *Journal of Geophysical Research*, *113*, D13204. https://doi.org/10.1029/2007JD008782

Zaveri, R. A., Easter, R. C., & Peters, L. K. (2005b). A computationally efficient multicomponent equilibrium solver for aerosols (MESA). *Journal of Geophysical Research*, *110*, D24203. https://doi.org/10.1029/2004JD005618

Zaveri, R. A., Easter, R. C., & Wexler, A. S. (2005a). A new method for multicomponent activity coefficients of electrolytes in aqueous atmospheric aerosols. *Journal of Geophysical Research*, *110*, D02201. https://doi.org/10.1029/2004JD004681